water

MDPI

Article

Large-Scale Particle Image Velocimetry for Estimating Vena-Contracta Width for Flow in Contracted Open Channels

Alireza Fakhri *, Robert Ettema, Fatemeh Aliyari and Alireza Nowroozpour

Department of Civil and Environmental Engineering, Colorado State University, 1372 Campus Delivery, Fort Collins, CO 80523-1372, USA; Robert.Ettema@colostate.edu (R.E.); Fatima.Aliyari@colostate.edu (F.A.); anowr@rams.colostate.edu (A.N.)

* Correspondence: Alireza.Fakhri@colostate.edu

Abstract: This paper presents the findings of a flume study using large-scale particle velocimetry (LSPIV) to estimate the top-width of the vena contracta formed by an approach open-channel flow entering a contraction of the channel. LSPIV is an image-based method that non-invasively measures two-dimensional instantaneous free-surface velocities of water flow using video equipment. The experiments investigated the requisite dimensions of two essential LSPIV components—search area and interrogation area– to establish the optimum range of these components for use in LSPIV application to contractions of open-channel flows. Of practical concern (e.g., bridge hydraulics) is flow contraction and contraction scour that can occur in the vena contracta region. The study showed that optimum values for the search area (SA) and interrogation area (IA) were 10 and 60 pixels, respectively. Also, the study produced a curve indicating a trend for vena-contracta width narrowing with a variable ratio of approach-channel and contracted-channel widths and varying bed shear stress of approach flow.

Keywords: LSPIV; contracted open channels; vena contracta width; search area; interrogation area

Citation: Fakhri, A.; Ettema, R.; Aliyari, F.; Nowroozpour, A. Large-Scale Particle Image Velocimetry for Estimating Vena-Contracta Width for Flow in Contracted Open Channels. *Water* **2021**, *13*, 31. https://dx.doi.org/10.3390/w13010031

Received: 6 November 2020
Accepted: 23 December 2020
Published: 26 December 2020

1. Introduction

Flow measurement provides crucial information for various hydraulics applications related to flow in bodies of water, e.g., dispersion of pollutants in rivers and coastal areas and problems associated with erosion, sedimentation, flooding, environmental degradation, and ice mitigation schemes [1]. Large-scale image particle velocimetry (LSPIV) is increasingly used to provide instantaneous and average velocities at the water surface of a flow. The method has been used on various hydraulic applications, such as flash-flood measurements [2–6], river and stream surface-flow measurements [7–10], and assessing debris-flow velocities in the field [11]. However, for certain flow situations, several unaddressed questions are associated with LSPIV. Notably, the LSPIV application requires guidance regarding the necessary size of the interrogation area (IA) to be used. IA is a square area incorporating the tracer particles and suitably large to encompass the scales of interest within the contracted flow field. Relatedly, in these same flow situations, LSPIV lacks guidance on the size of the search area (SA), a rectangle with the same center as the IA but extending beyond the IA to encompass flow directions with designated accuracy.

This paper reports findings of experiments to evaluate requisite values of IA and SA needed when using LSPIV to estimate the top-width of a vena contracta formed when an open-channel approach flow enters a contraction in the channel's width. This study investigated flows into contracted open channels, with the contraction ratio defined as contracted-channel width (B_2) divided by approach-channel width (B_1) [12]. Three contraction ratios were used: B_2/B_1 = 0.25, 0.50 and 0.75. The vena contracta of a contracted flow is the narrowing of flow as it passes through a contracted area of flow before eventually spreading downstream to occupy the contracted channel's full width. This effort entailed evaluating the sensitivity of LSPIV components IA and SA to establish the optimum size

range of these components for use in image processing of open-channel flows that contract. A thorough search of the relevant literature yielded that LSPIV has not been used for vena-contracta widths in open-channel flow contractions.

2. Background

Here, a brief background is given about the LSPIV method and vena-contractas formed in open-channel contractions. Whereas LSPIV is quite extensively documented, vena-contracta formation is entirely absent from textbooks on open channel-flows [12].

2.1. Large Scale Particle Image Velocimetry

LSPIV is an image-based methodology that non-intrusively measures two-dimensional, instantaneous free-surface velocities of water flow using standard, inexpensive video equipment. LSPIV is recognized as being a robust means of indenting the flow field at the water surface [13]. The method is assumed applicable when the flow pattern examined is at least an order of magnitude larger than turbulence scales in the large water body [14], and has certain advantages compared with other types of velocity measurement instruments, such as acoustic Doppler velocimeters (ADV) and particle image velocimetry (PIV). The use of ADV requires placement of the instruments directly in the flow field, which seems cumbersome in big rivers with unsteady flow fields. Moreover, the ADV method only measures velocity at a single point, whereas LSPIV can provide a two-dimensional flow pattern at the water surface. Another advantage of LSPIV over conventional instruments, such as ADV, is that LSPIV can be used for shallow flows, whereas ADV requires 0.25 m minimum water depth [15]. Additionally, LSPIV can cover larger flow fields such as flood flow [16] and can be easily used with readily available illumination devices and video equipment.

In LSPIV, sequential images of river surface flow viewed from a riverbank or a bridge are sampled at a specific time interval and utilized to extract quantitative flow information [16]. In the next step, the captured images are ortho-rectified using a mapping relation between the image coordinates and the physical coordinates with additional water surface level information [16]. Ortho-rectification is the process of removing the effects of image perspective and relief effects for the purpose of creating a planimetrically correct image with a constant scale wherein features are represented in their proper positions. LSPIV applies a cross-correlation statistical method on the orthro-rectified images to measure the displacements of the tracer particles. The accuracy of the method varies on a case-by-case basis and depends highly upon the geometry and the flow field of interest. Furthermore, in some situations, the application of LSPIV is difficult, and the results for flow patterns and velocity vectors estimated may have a high level of errors. Currently, information on the source of errors and uncertainties is scarce, and a typical measurement-based investigation cannot estimate all types of errors [16]. Therefore, in this application, two critical parameters, interrogation area (IA) and search area (SA), are selected to be investigated to find the optimum range of parameters in terms of the velocity magnitude and flow mapping.

The two critical parameters for calculating tracer velocities are the interrogation area (IA) and search area (SA). The interrogation area (IA) is a square area that incorporates all the tracer particles and can be representative of the scales of interest within the flow field. The interrogation area (IA) must be large enough to incorporate tracers but small enough to represent the flow (velocity gradient in an IA must be negligible). The search area (SA) is a rectangle defined around the center of the interrogation area. It corresponds to the zone in which the patterns are searched on the successive images [17].

In this study, the software FUDAA-LSPIV [18] was used to convert video images and calculate velocity vectors. FUDAA-LSPIV is an open-source French software developed by EDF and Irstea, based on previous scientific works on the LSPIV technique. FUDAA-LSPIV was implemented under the GPL license as a user-friendly Java graphical interface that calls Fortran solvers [19]. The version used in this experiment is Version 1.6.2. This version can

determine streamlines, flow discharge, and can transform images to PNG format without using additional software, making it a very user-friendly software.

2.2. Vena Contracta in Open-Channel Flow

A vena contracta develops when flow narrows and separates from the flow's boundaries as it passes into a contracted area of flow. In free-surface flows, vena contractas are often reported for flows entering spillways and outlets, e.g., for free- and submerged-flow discharges through ungated and gated spillways [20,21]. For example, previous studies included investigations of a vena contracta formed when flow passed beneath sluice or spillway gates [22]. Vena contractas often form within reservoir outflow ducts [23] and for flow along pressurized conduits with geometry changes [24]. The vena contracta width and depth were measured with different methodologies, e.g., dye tracers and dye injections [25,26], and Particle Tracking Velocimetry (PTV) [27]. However, a substantial gap in the literature [12] exists regarding vena-contracta formation within a contraction entrance of open channels and how the dimensions of such vena contractas vary with channel geometry and flow conditions. This gap has significance for understanding flow through bridge waterways. LSPIV is a seemingly convenient method to gain information on the top-width of a vena contracta formed by an approach open-channel flow entering a contraction of the channel. Moreover, it is more convenient than alternative methods like ADV measurements or dye as it readily applicable, provided suitable magnitudes of IA and SA are selected to facilitate LSPIV accuracy.

3. Experiment Setup and Procedure

The experiments were conducted using a flume in the Hydraulics Laboratory at Colorado State University. This flume was 2.44-m-wide, 60.96-m-long, and 1.22-m-deep, and fitted with two adjustable internal walls placed along the flume. The moveable walls enabled three different contraction ratios to be used. Fine sand was used to cover the bed to a depth of 0.46 cm. Three different contraction ratios were used: tight (B_2/B_1 = 0.25); medium (B_2/B_1 = 0.5); and modest (B_2/B_1 = 0.75). The contracted channels are illustrated in Figure 1.

Figure 1. Views of the contracted flume for three different contraction ratios: (**a**) B_2/B_1 = 0.25; (**b**) B_2/B_1 = 0.50; (**c**) B_2/B_1 = 0.75.

For the scour study on this flume, a combination of 31 different discharges and situations were tested, and 19 runs were selected for the LSPIV investigations. Table 1 indicates the operations used for LSPIV and includes information about the corresponding discharge and contraction ratio for each experiment. The scour study on this flume consists of three different conditions, live bed (LB), clear water (CW), and Fixed bed (FB) that are listed in Table 2. The present study was a collaborative work with a contraction scour study on rectangular channels [28].

Table 1. Abbreviation table.

Abbreviation/ Symbols	Definition
B_1 (m)	The width of the approach channel
B_2 (m)	The width of the contracted channel
B'_2 (m)	The minimum width of the vena contracta
CW	Clear Water
FB	Fixed Bed
Fr	Froude number of the uniform approach flow
GRP	Ground Reference Point
IA	Interrogation Area
K_v	Vena Contracta Coefficient
LW	Live Bed
SA	Search Area
Sim	The distance from the top of the search area to the center
Sip	The distance from the bottom of the search area to the center
Sjm	Distance from the upstream side of the search area to the center
Sjp	The distance from the downstream side of the search area to the center
τ_1 (N/m^2)	Shear stress
τ_c (N/m^2)	Shear stress for incipient motion

Table 2. Test conditions and their corresponding discharge (Q) and contraction ratio (B_2/B_1).

Test Condition	Contraction Ratio (B_2/B_1)	Discharge Q (CMS)
LB	0.75	0.190
LB	0.75	0.231
CW	0.75	0.111
LB	0.75	0.161
LB	0.75	0.138
LB	0.75	0.288
CW	0.75	0.099
CW	0.25	0.064
CW	0.25	0.087
LB	0.5	0.231
LB	0.5	0.161
LB	0.5	0.190
LB	0.5	0.138
CW	0.5	0.064
CW	0.5	0.076
CW	0.5	0.087
FB	0.25	0.064
FB	0.25	0.092
FB	0.25	0.076

Two sizes of paper tracers were used as seed particles: 1 mm tracers and 2 cm tracers. The tracers were easy to observe by the video camera and ecologically inert. For the seeding part of each experiment, an adequate number of particles were used to provide enough tracer coverage for at least fifteen seconds and proper coverage of the whole flow field.

A requirement for suitably accurate LSPIV is the acquisition of a detailed video image. An OLYMPUS-10 4K camera was used for capturing videos; all the videos were taken at 30 frames per second (30 HZ), an adequate sampling rate for capturing velocities in hydraulic applications [13]. Also, it was essential to avoid camera vibration and light reflection on the water surface. To avoid such problems, the camera was set on a tripod, and the absence of possible light reflection from the water surface was checked. The camera's tilting angle was 45 degrees to minimize the distortion during the image processing, which is a reasonable angle for the camera when the minimum acceptable limit is 10 degrees [29].

LSPIV requires the use of benchmarks (GRP) to locate the flow and enable ortho-rectification of the video image, which was taken at an oblique angle. A minimum of 6 benchmarks is required for image transformation and orthorectification [13]. In this study, 10 GRPs were selected for each application. Figure 2 shows the chosen GRP locations for the 0.75 contraction ratio.

Figure 2. Locations of GRPs for 0.75 contraction ratio. The locations are designated as P1 through P10.

As mentioned above, the flume was designed to investigate the contraction scour. Most applications were conducted once the contraction had mainly attained an equilibrium condition. The time of capturing videos based on the equilibrium condition varies between 7 to 18 h.

Use of the FUDAA-LSPIV software involved the following steps in calculating flow velocities [17]:

1. Begin the software setup and select the video-record images;
2. Orthorectify the images and define each benchmark location;
3. Define an interrogation area and a search area;
4. Form the estimation grid; and,
5. Calculate the local velocity values at each position and then determine the average at each position.

The first step for using the LSPIV software entailed selecting a sequence of images in a video record. The video was uploaded in the software, and the beginning and the end of the video were then defined. For all the measurements, the number of frames per second was kept at 30. The number of images used for each measurement varied from 200 to 500 to find the best interval for which the paper tracers covered the entire flow field associated with flow passing through the contraction.

To get a suitably correct ortho-rectification of an image required the use of ten benchmark locations. These locations needed to be well distributed in the image. It then was possible to define the transformation parameter and use the software to calculate default values. The water-surface level variation was related to the benchmark locations. The next step entailed transforming all images based on the input data and calculating the velocities. The last step, after orthorectification, entailed checking the benchmark locations in each image. A risk associated with the method was that an image could be stretched, shrunk, or blurry after the ortho-rectification process. The ortho-rectified image for $B_1/B_2 = 0.5$ is represented in Figure 3.

Figure 3. The orthorectified image for contraction ratios of $B_2/B_1 = 0.5$.

The interrogation area (IA) is a square area that incorporates all the tracer particles and represents the scales of interest within the contracted flow field. The area should not be so large as to adversely affect the IA calculation efficiency and so small as to make the results insufficiently accurate. In this study, IA was varied from 20 pixels to 90 pixels.

The search area (SA) is a rectangle with the same center as the IA. It is an area that shows the basic flow patterns on a set of continuous images. The SA can be enlarged to ensure the results are suitably accurate for the study. Also, the SA is defined using four direction variables: Sim, Sip, Sjm, and Sjp (Figure 4).

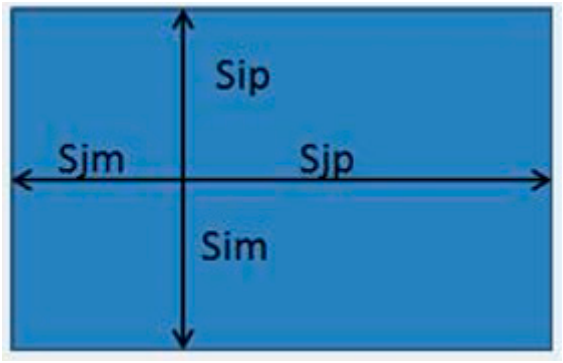

Figure 4. Sim, Sip, Sjm, and Sjp directions within a SA.

The brief definitions of variables are as follow:

Sim = The distance from the top of the search area to the center.
Sip = The distance from the bottom of the search area to the center.
Sjm = Distance from the upstream side of the search area to the center.
Sjp = The distance from the downstream side of the search area to the center.

One run from the modest contraction ratio (B_2/B_1 = 0.75) was selected to find the best values for IA and SA. This experiment had a discharge of 0.138 m^3/s, and the flow depth was 21.0 cm at the approach. To estimate the most accurate IA value, the other parameters- Sim, Sip, Sjm, and Sjp were kept 10 pixels initially. These initial values are selected according to Sutarto's research, in which the best value of Sim is 7 pixels for waterways with expansions [30]. Then, different values of IA, e.g., 90, 80, 60, 50, 40, 30, and 20 pixels, were assigned to measure the magnitude of velocity vectors. For comparing the accuracy of results, velocity vectors were measured by ADV at 28 points over the area of interest. These points were selected to cover the whole flow field, including approach, near walls, and the contracted area. The selected points and their locations are illustrated in Figure 5. The findings from LSPIV were then compared with the ADV results to find the most accurate value for IA. In the next step, the best value of IA was kept constant, and the SA components were selected, e.g., Sim, Sip, Sjm, and Sjp = 5, and 15. Finally, the values of IA and SA with the minimum error were used for the rest of the experiments.

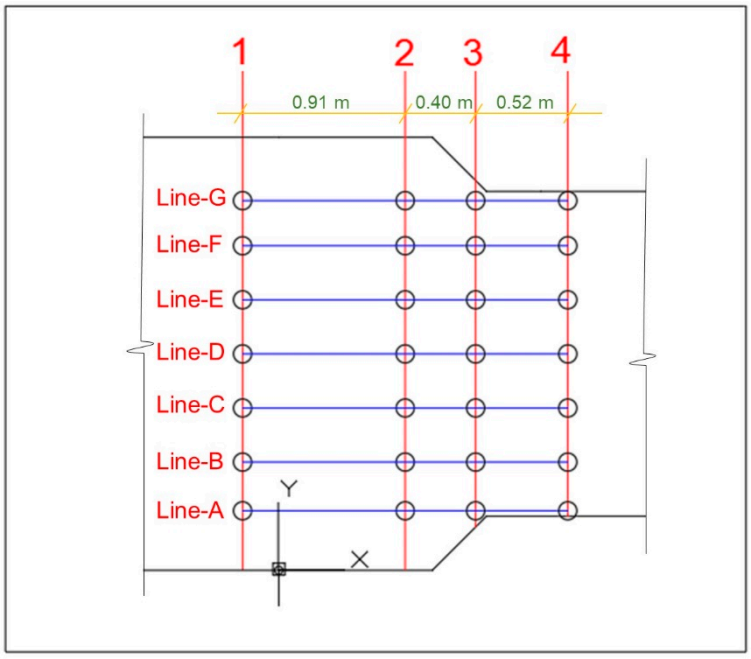

Figure 5. Selected points for the ADV data collection.

For each data collection by ADV, the flow depth was measured by using an acoustic sensor, and the velocities were collected at 0.6 of the flow depths. The velocity at 0.6 flow depth gives the average velocity, and to estimate the surface velocities by ADV; it was assumed that the mean velocity in a vertical profile is 80–90% of the water surface velocity [31]. Then, all the ADV data were adjusted to compare with the LSPIV findings. The measured free-surface velocities with a basic LSPIV system have uncertainties ranging between 10% and 35% (at 95% confidence level) [16]. In this study, 15% precision was selected as the acceptable level of accuracy to compare ADV and LSPIV measurements.

4. Results and Discussion

The results comprise findings regarding the IA and the SA, and then the findings regarding the trend for flow contraction through the vena contracta formed in a contracted open channel. Figure 6 is an example of selected IA, SA, and their location when B_2/B_1 = 0.5.

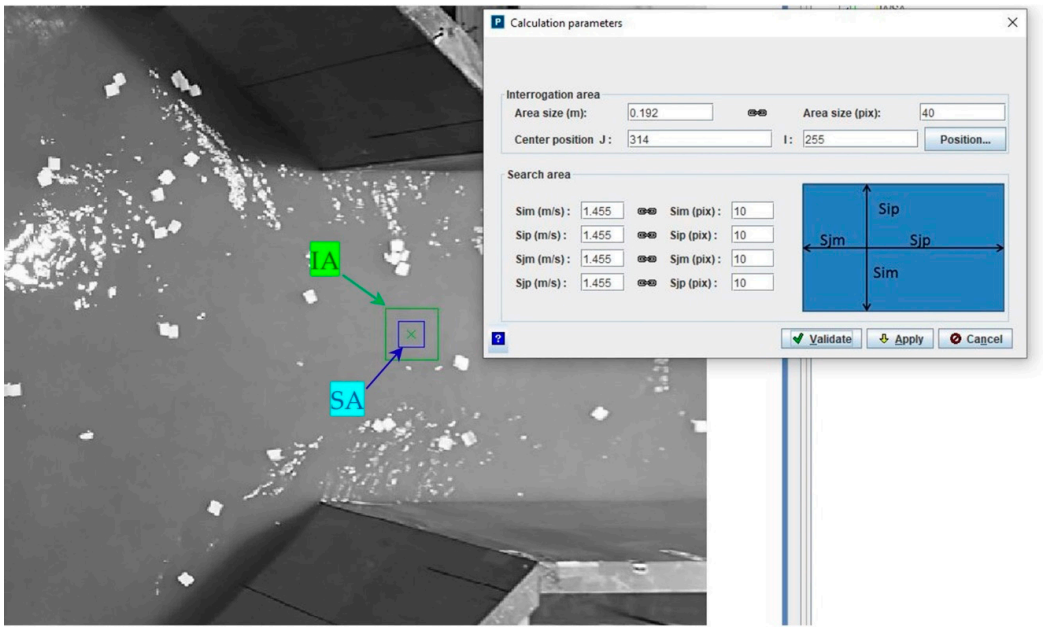

Figure 6. Delineation of the search area (SA) and the interrogation area (IA).

4.1. Interrogation Area and Search Area Values

The results for different values of IA at the centerline of the flume (Line-D) are shown in Figure 7. In this plot, the black line indicates the measured velocities by ADV at the centerline. This plot demonstrates that the velocities measured by LSPIV, when IA is between 40 to 80 pixels, have the minimum range of errors between 1% to 5%, and the best value of IA is 80 pixels. Furthermore, it can be concluded that the IA range between 40 and 80 pixels still have an acceptable level of accuracy. Figure 8 shows the measured velocities in the vicinity of the centerline (line-C). Velocities calculated using LSPIV indicate that the precision is acceptable when IA is above 50 pixels, and it is insensitive to any change in values of IA greater than 50 pixels. Also, it implies that the maximum errors occur at point C1, where the tracers enter the flow region. Figure 9 shows the measured velocities at line-B, showing that the measured velocities are insensitive to change in the value of IA, and smaller values of IA give a better result at regions where the velocity gradient is high.

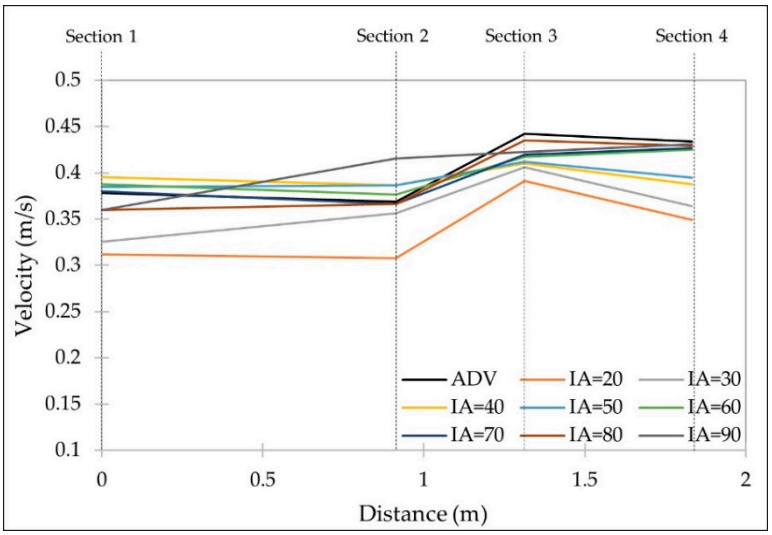

Figure 7. Measured Velocities obtained using LSPIV and ADV at Line-D (see Figure 5).

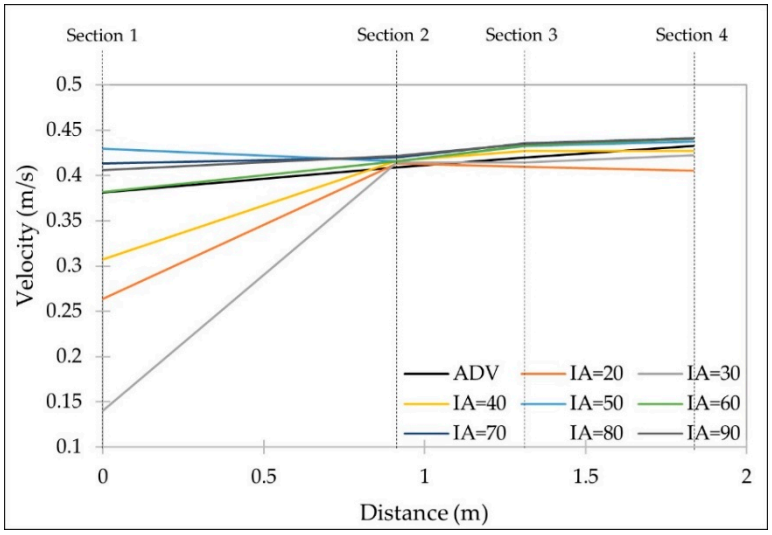

Figure 8. Measured Velocities obtained using LSPIV and ADV at Line-C (See Figure 5).

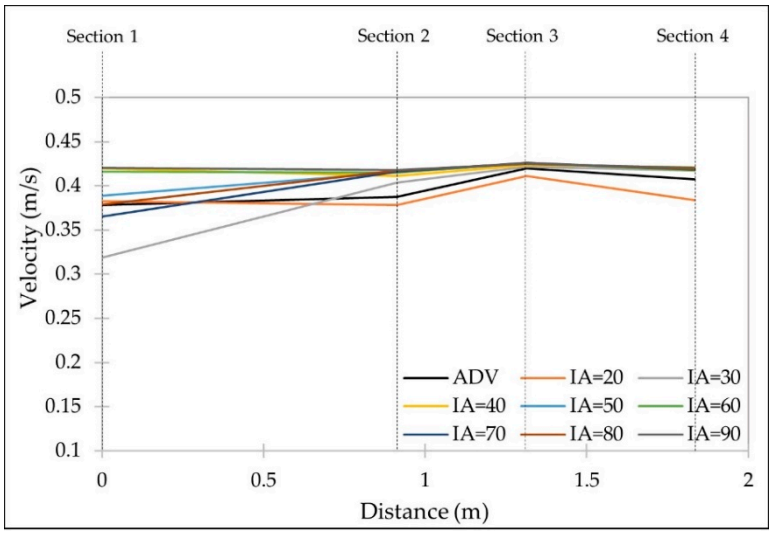

Figure 9. Measured velocities obtained using LSPIV and ADV at Line-B (See Figure 5).

Also, it can be concluded that the maximum occurs where the tracers enter the flow region. Figure 10 depicts the velocities near the wall (Line-A). This plot reveals that the measured velocity vectors have the maximum accuracy when IA is within 30 and 90 pixels, and between this range, the results are insensitive to change of IA. Moreover, this plot shows that the measured velocities by LSPIV differ from ADV and the level of error increases where particles reach the contraction. The possible reasons for the differences are the high-velocity gradient and tracer particles being close to the boundaries.

The IA value was selected to be 80 pixels in the next step, and different values for SA then were set. The sensitivity of SA was investigated at the centerline (Line-D). Figure 11 represents the results for IA = 80 pixels and SA = 5, 10, 15 pixels. This plot indicates that the measured velocities by LSPIV have an acceptable range of errors when SA's value is below 10 pixels. Furthermore, values of SA higher than 10 pixels have a significant increase in computational time.

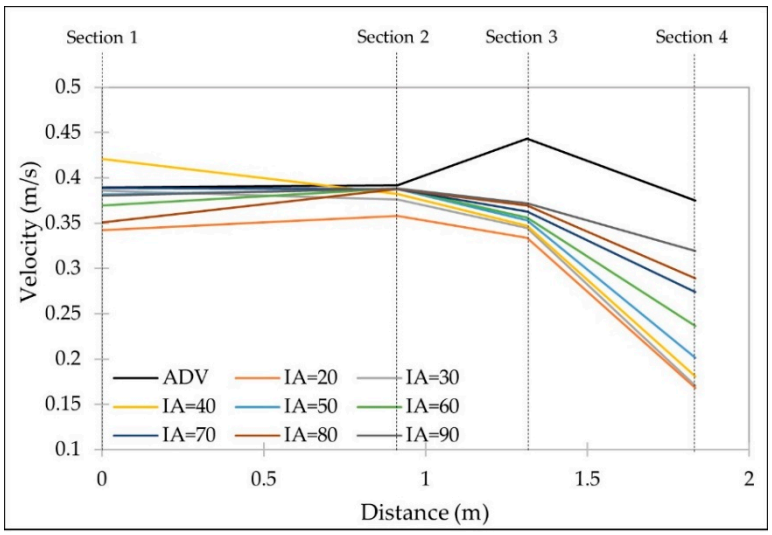

Figure 10. Measured velocities obtained using LSPIV and ADV at Line-A (See Figure 5).

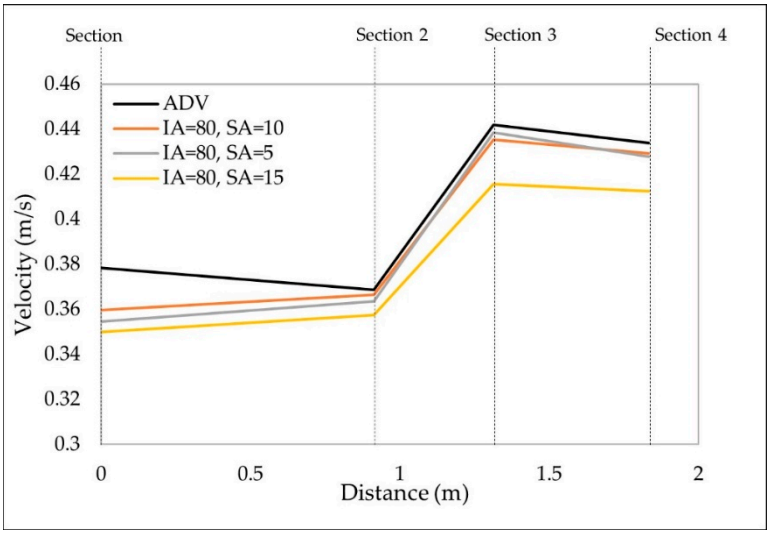

Figure 11. The sensitivity of measured velocities to SA at the centerline (Line-D).

4.2. Flow Mapping

The results from the previous section indicate that selecting IA between 40 to 80 pixels can accurately determine the velocity vectors and streamlines for lines B, C, and D, and precision is higher when IA is 80 pixels. For line A, when the flow reaches the contraction and near the walls, drawing the streamlines showed that LSPIV could precisely map the flow when IA is 60 pixels. For having a clear definition of the overall flow pattern, especially near the walls and contraction, IA and SA were selected 60 and 10 pixels, respectively. This selection has an adequate precision for measuring velocities, and it can map the flow pattern precisely. The capability of flow mapping by LSPIV when IA is 80, and 60 pixels are compared in Figure 12. This figure reflects some errors in drawing the streamlines at the tip of contraction when IA is equal to 80 pixels

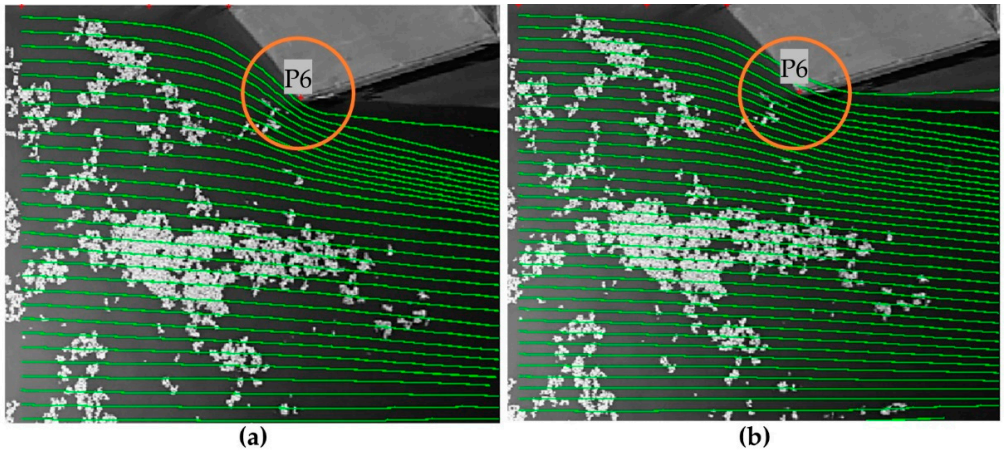

Figure 12. The flow field in a contraction when B_2/B_1 = 0.75: (**a**) streamlines when IA = 60 pixels; (**b**) streamlines when IA = 80 pixels.

With the selected values of IA and SA, the remaining 19 tests were conducted to plot the streamlines. The defined streamlines and the velocity vectors by LSPIV for the contraction ratio of 0.25, and the discharge of 0.064 m^3/s, is depicted in Figure 13a,b, respectively. This figure shows that setting the LSPIV parameters to IA = 60 and SA = 10 can accurately map the flow pattern. Furthermore, the velocity vectors were drawn correctly in terms of magnitude and direction.

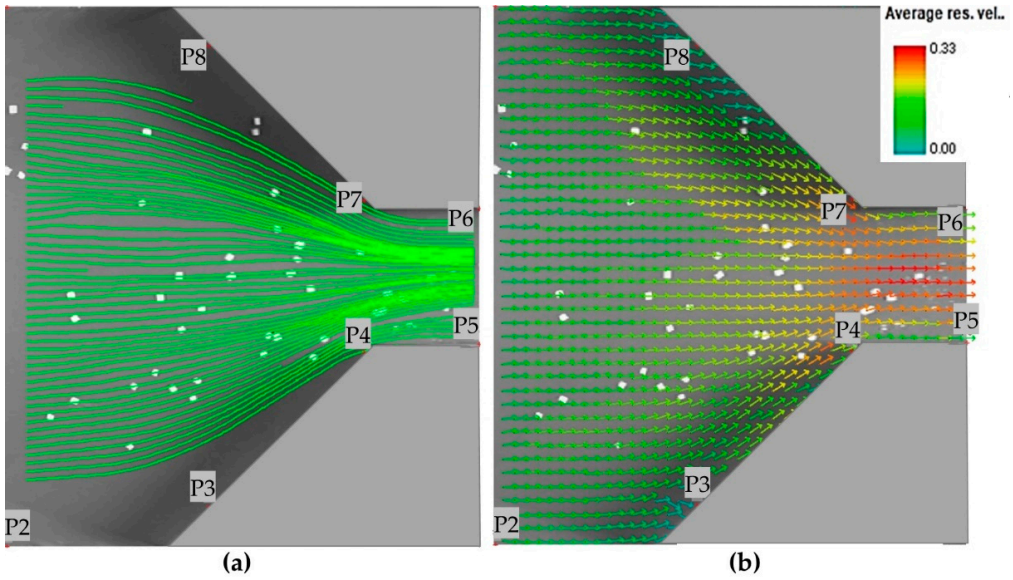

Figure 13. (**a**) Streamlines and (**b**) velocity vectors for Q = 0.064 m^3/s and B_2/B_1 = 0.25.

Figures 14 and 15 illustrate the streamlines and velocity vectors for 0.5 and 0.75 contraction ratio when the discharges are 0.076 m^3/s and 0.128 m^3/s, respectively. These figures indicate that the selected parameters can adequately determine the flow pattern and velocity vectors for different contraction ratios.

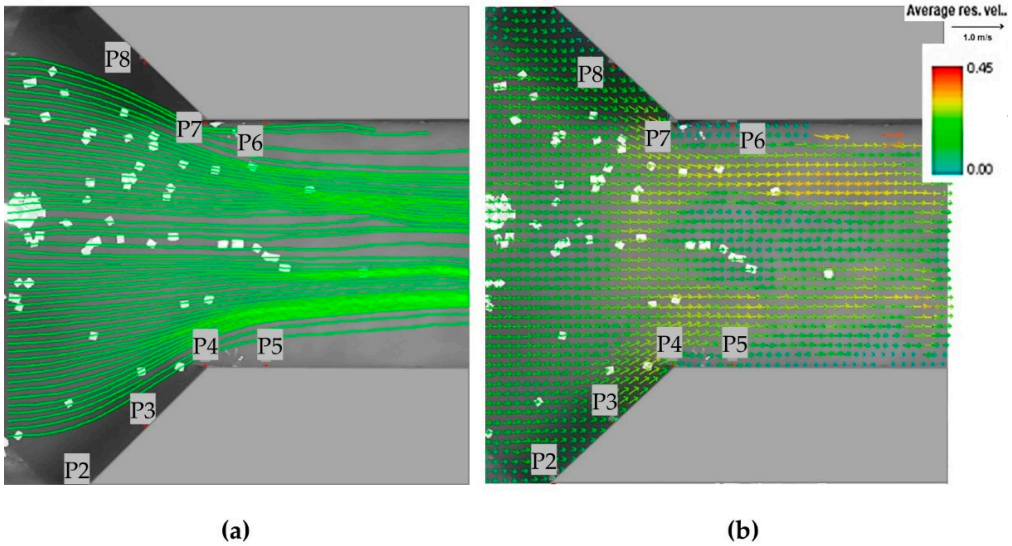

Figure 14. (**a**) streamlines and (**b**) velocity vectors for $B_2/B_1 = 0.5$ and $Q = 0.23\ m^3/s$.

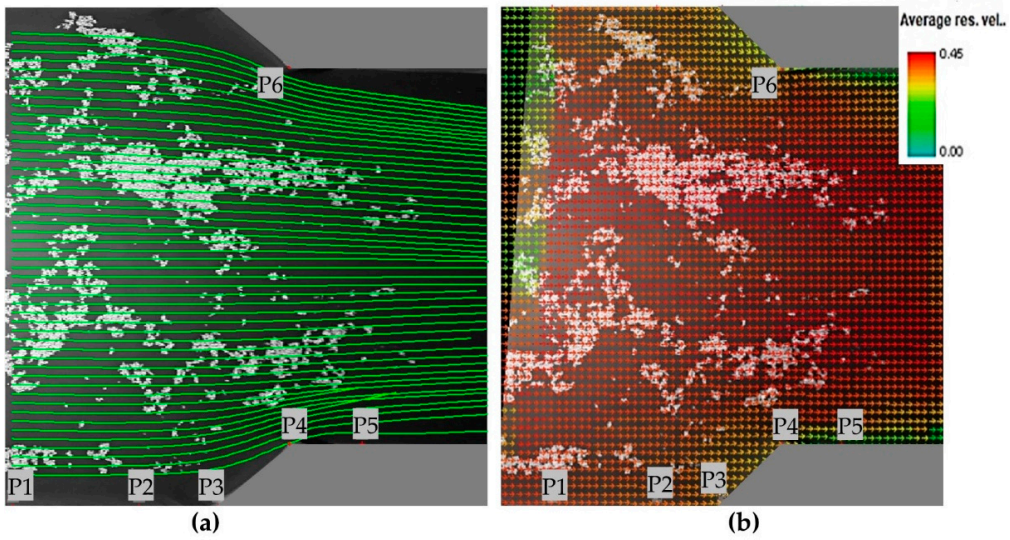

Figure 15. (**a**) Streamlines and (**b**) velocity vectors for $B_2/B_1 = 0.75$ and $Q = 0.138\ m^3/s$.

4.3. Values of Vena-Contracta Width

The FUDAA Version 1.6.1 software enables the calculation of the streamlines in the flow field, which can be used for delineating the top of a vena contracta. In this step, therefore, a straight line was drawn transverse across the flow to indicate the flow field from which streamlines were to be drawn. For the present application of the FUDAA software, the straight line was drawn at the contraction's entrance cross-section. The defined line for $B_1/B_2 = 0.5$ and discharge = $0.23\ m^3/s$, and the corresponding streamlines are shown in Figures 16 and 17, respectively.

The different contraction ratio values results, B_1/B_2, and discharges were then uploaded into an AutoCAD file. Later, all the images were scaled, and the vena contracta width B'_2 was measured. The following variables were used in this process:

B_1 = the width of the approach channel
B_2 = the width of the contracted channel
B'_2 = the minimum width (the width) of the vena contracta
V = velocity of uniform approach flow upstream of contraction
Y = depth of uniform approach flow upstream of contraction
Fr = Froude number of the uniform approach flow

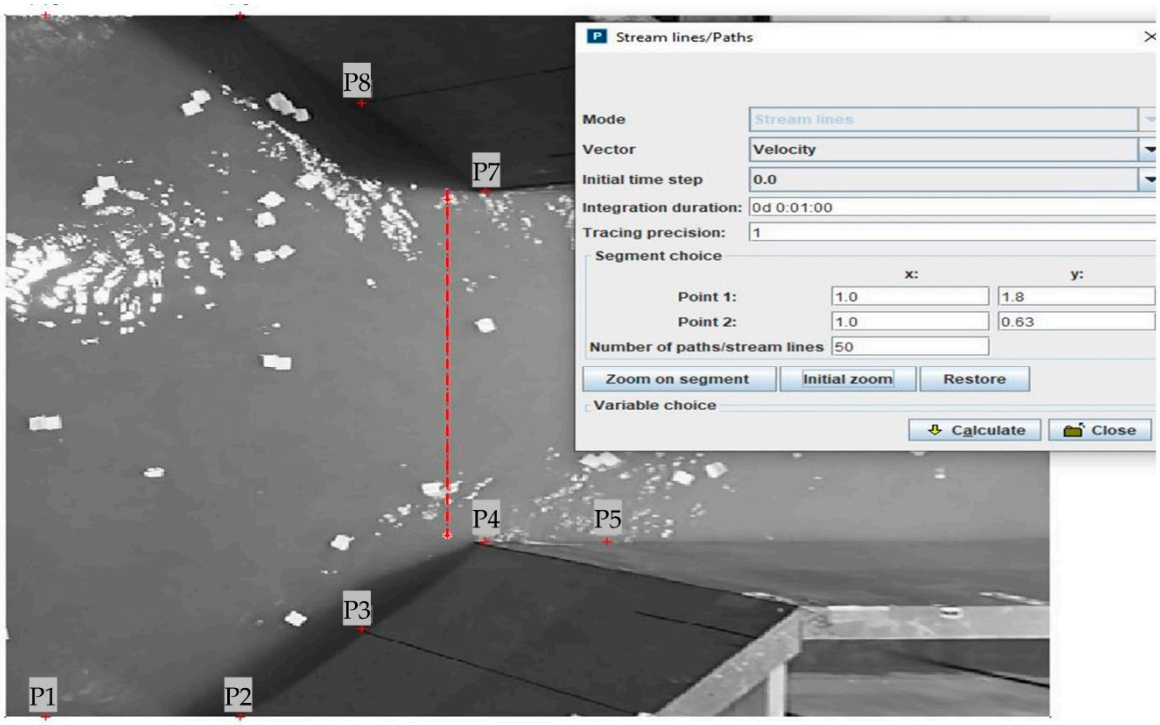

Figure 16. The defined transverse line is used for calculating the streamlines.

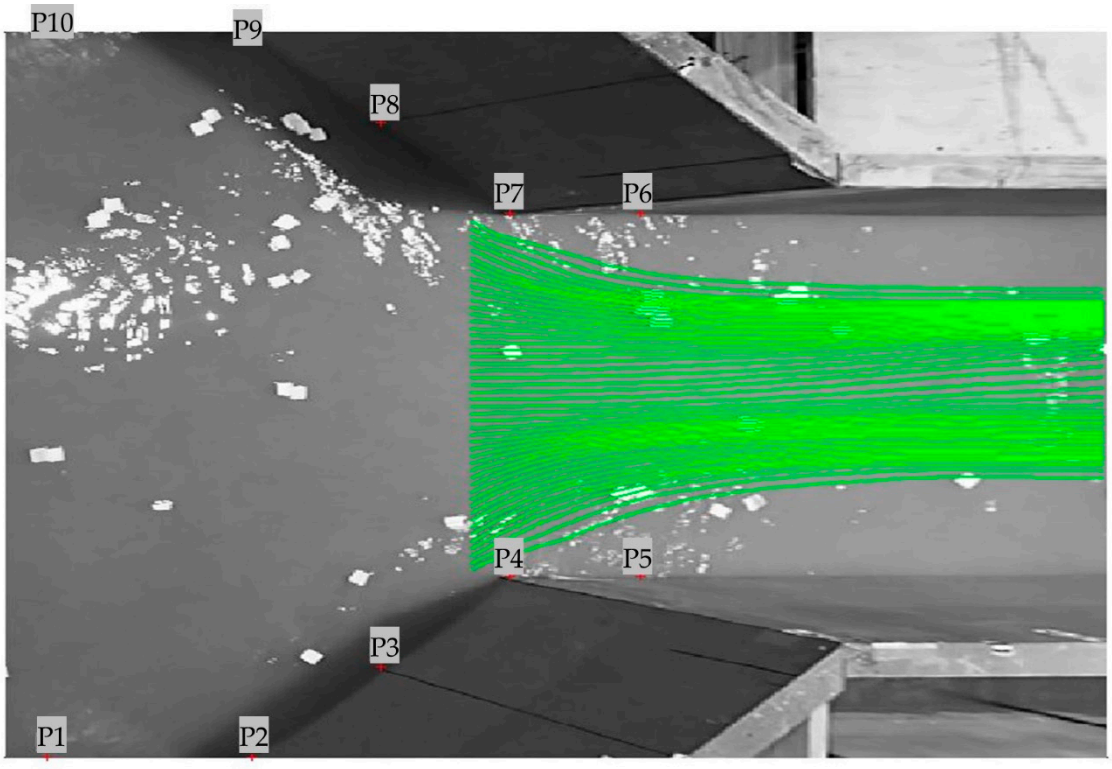

Figure 17. Calculated streamlines obtained for B_1/B_2 = 0.5 and discharge = 0.23 m^3/s.

Figure 18 is an illustrative example of the (minimum) vena contracta width estimated for B_2/B_1 = 0.5 and Q = 0.23 m^3/s. This figure shows the dimensions of the flow entering the contracted channel and the main dimensions measured using the LSPIV technique.

Some other example results for the other contraction ratios and discharges are presented in Figures 19 and 20.

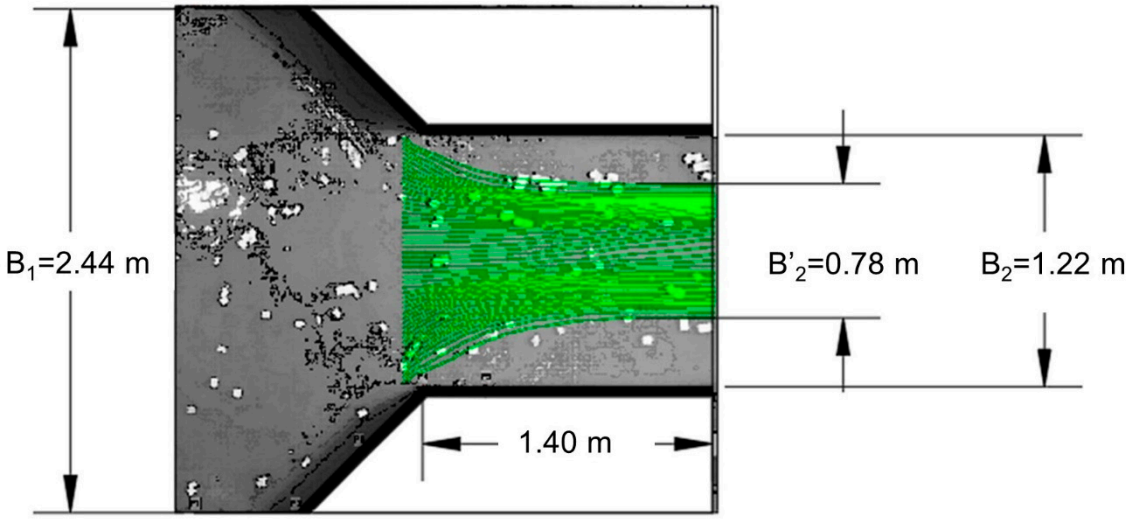

Figure 18. The measured value of vena contracta width B'_2 obtained for experiment with $B_2/B_1 = 0.5$ and discharge of 0.23 m^3/s.

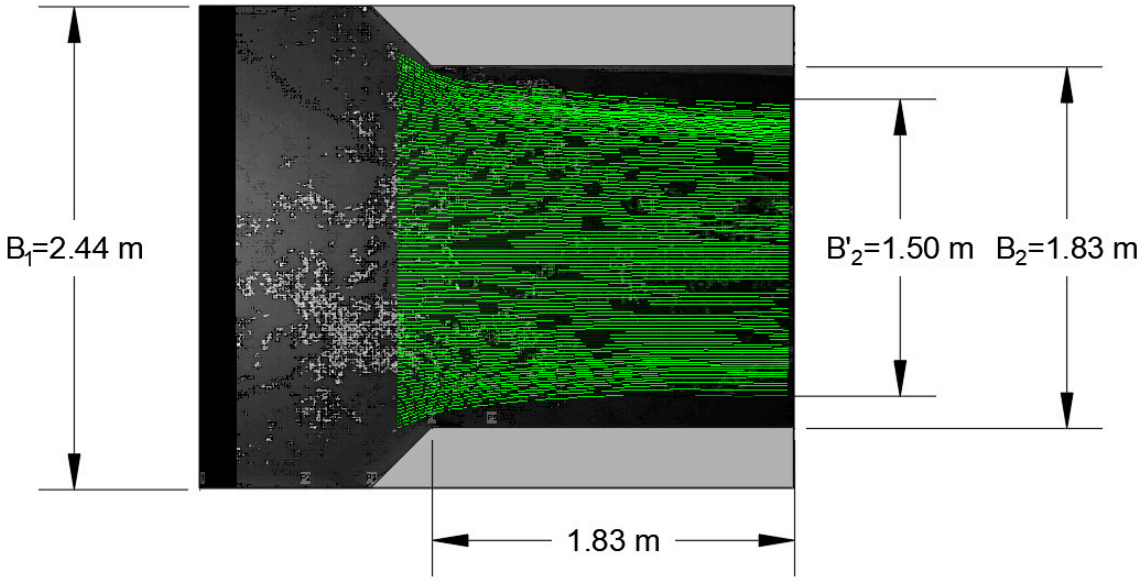

Figure 19. The measured value of vena contracta width B'_2 obtained for experiment with $B_2/B_1 = 0.75$ and discharge of 0.099 m^3/s.

The results from LSPIV measurements for the ranges B_2/B_1 and τ_1/τ_c in the flume experiments were examined to estimate vena contracta coefficient $K_v = B'_2/B_2$ for the entrance configurations tested. The results for K_v were plotted as the two curves depicted in Figure 21. Table 3 gives the measured vena contracta ratios estimated for all the experiments. The values of K_v were determined at the end of each experiment. To aid scour estimation, the values (Figure 21) corresponded to equilibrium scour conditions within the contraction. Also, three values of K_v were estimated for the tight contraction, $B_2/B_1 = 0.25$, when the contracted channel's bed was fixed flat. Values of K_v also were determined for the initial conditions of runs with $B_2/B_1 = 0.25$. The trends in Figure 21 show that the measured top width of vena contracta decreases asymptotically as the abscissa term $(B_1/B_2 - 1)$ Fr

increases. This nondimensional term describes the narrowing of the vena contracta for increased approach-flow velocities expressed as $Fr = V/(gY)^{0.5}$. It cannot be bolstered by theoretical prediction because of the generation of oscillatory turbulence structures in the regions of flow separation, causing the vena-contracta to form. The lower curve in Figure 21 indicates that, before scour enlarging of the flow cross-sectional area, the vena-contracta width was less than after scour. The upper curve is of more use when estimating bridge-waterway scour because scour equilibrium is based upon flow area at equilibrium scour depth.

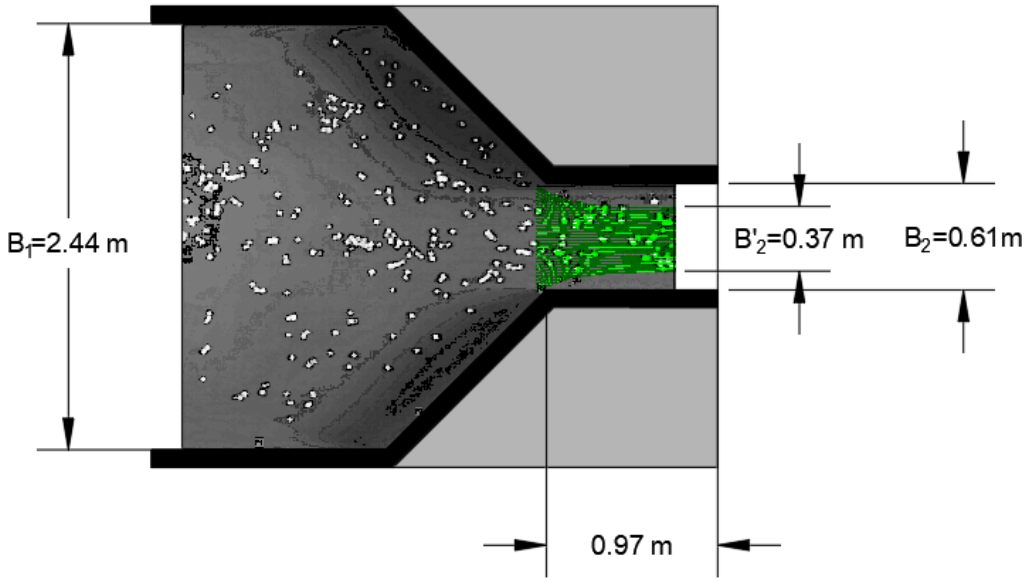

Figure 20. The measured value of vena contracta width B'_2 obtained for experiment with $B_2/B_1 = 0.25$ and discharge 0.087 m^3/s.

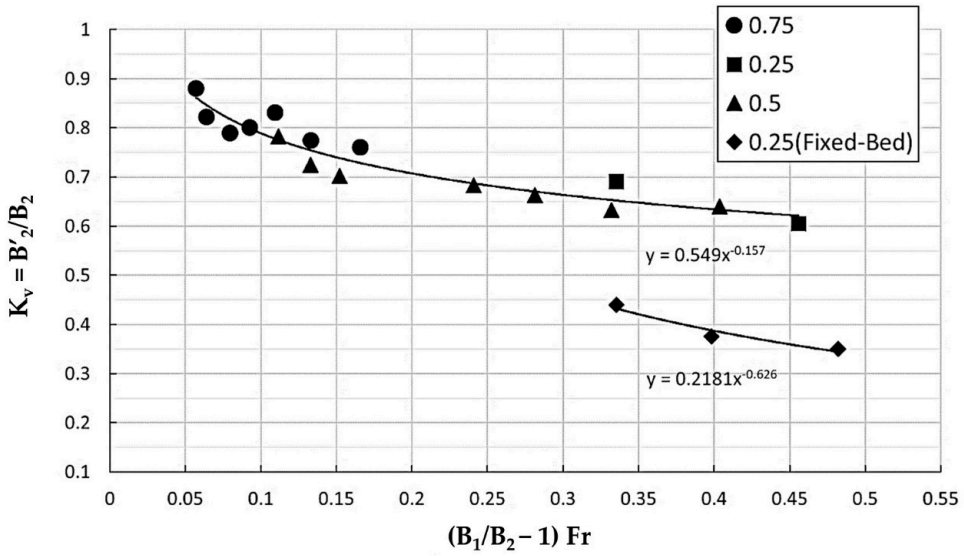

Figure 21. Values of vena-contracta coefficient, K_v, for a loose boundary channel with a 45° channel entrance. Two curves are shown: the fixed bed indicates the value of K_v before contraction-scour developed. Displayed in the legend box are the values of B_2/B_1.

Table 3. Estimated vena contracta ratios and details for all experiments.

Test Condition	Contraction Ratio (B2/B1)	Discharge Q (CMS)	B'_2 (m)	(B'_2/B_2)	V (m/s)	Fr	$(B_1/B_2 - 1)$ Fr
LB	0.75	0.190	1.52	0.83	0.44	0.332	0.109
LB	0.75	0.231	1.41	0.77	0.53	0.403	0.133
CW	0.75	0.111	1.50	0.82	0.26	0.194	0.064
LB	0.75	0.161	1.46	0.80	0.37	0.281	0.093
LB	0.75	0.138	1.44	0.79	0.32	0.241	0.079
LB	0.75	0.288	1.39	0.76	0.66	0.503	0.166
CW	0.75	0.099	1.61	0.88	0.23	0.173	0.057
CW	0.25	0.064	0.42	0.69	0.15	0.112	0.335
CW	0.25	0.087	0.37	0.61	0.20	0.152	0.456
LB	0.5	0.231	0.78	0.64	0.53	0.403	0.403
LB	0.5	0.161	0.81	0.66	0.37	0.281	0.281
LB	0.5	0.190	0.77	0.63	0.44	0.332	0.332
LB	0.5	0.138	0.83	0.68	0.32	0.241	0.241
CW	0.5	0.064	0.95	0.78	0.15	0.112	0.112
CW	0.5	0.076	0.88	0.72	0.17	0.133	0.133
CW	0.5	0.087	0.86	0.70	0.21	0.152	0.152
FB	0.25	0.064	0.27	0.44	0.15	0.112	0.335
FB	0.25	0.092	0.21	0.35	0.21	0.161	0.482
FB	0.25	0.076	0.23	0.37	0.17	0.133	0.398

5. Limitations

Besides the limitations inherent in selecting suitable values of SA and IA (as discussed above), LSPIV was found to become less accurate for estimating velocities of flow in regions where the flow developed waviness, though LSPIV still was sufficiently accurate for the purpose of estimating the minimum width of a vena contracta. The vertical fluctuations of flow decreased the estimated magnitudes of velocity by lengthening the flow path by including an upward and downward component. This limit was noticeable when the contraction ratio $B_2/B_1 = 0.25$, in which standing waves formed. Though the estimated width of vena contracta was sufficient (agreed with observations by eye), the velocities were less than values estimated from the velocity profile obtained using ADV.

Another limitation documented elsewhere [1] is that the tracer particles must be suitably small to delineate flow structures visible on the water surface. This limitation was addressed in the study and led to selecting the tracer size used, as mentioned above. Under these conditions, the turbulence from the separation zones at the entrance corners caused the vena-contracta boundaries to oscillate. Small standing waves developed from the entrance corners led the tracer particles to move up and down when passing into the contracted channel. Therefore, the use of LSPIV in conditions where the water-surface was wavy did not result in reliable estimates of velocity at the flow surface. However, the estimates of B'_2 were considered sufficiently useful to complete the trends shown in Figure 21.

6. Conclusions

LSPIV is a useful and readily applicable way to illuminate flow patterns at water-surfaces, and indeed to obtain estimates of flow velocities at the water surface. Such water surfaces must be planar, however, if flow velocities are to be assessed. The present study focused on LSPIV use for estimating the narrowest width of vena contractas formed in open-channel contractions, and particularly on the influences consequent to selecting the search area (SA) and interrogation area (IA) when applying LSPIV. These foci are missing from the literature on LSPIV use.

This study indicates that SA should be between five and 10 pixels, and that SA is insensitive to values above 10 pixels. However, values higher than ten pixels increase the computational time significantly.

The IA values should exceed 80 pixels to give acceptable accuracy (for the present study) when the region is straight, with no contraction. The level of accuracy declines at boundaries and when the velocity gradient is high. When the velocity gradient is high and the flow faces a contraction, IA = 60 gives a better precision in terms of magnitude and mapping the streamlines. Results from the IA investigations reveal some errors where the flow enters the interest area. To overcome this limitation, it is recommended that the grid lines at the entrance be extended to increase the level of accuracy in the area of interest.

The maximum accuracy obtainable using LSPIV, this study suggests that researchers should consider the flow conditions to select appropriate SA and IA values. When finding the velocity magnitude is of interest with a low level of velocity gradient, IA = 80 pixels, and SA = 10 can be used. When the flow is wavy, and the flow mapping is essential, IA = 40–60, and SA = 10 can be a convenient choice for the LSPIV parameters.

LSPIV was found useful for estimating the values of the minimum width of the vena contracta in an open-channel contraction. However, its use required judgment for the higher discharges through the smallest value of B_1/B_2 used (0.25).

Author Contributions: Conceptualization, A.F., and R.E.; methodology, A.F., and R.E.; validation, A.F., R.E., and A.N.; formal analysis, A.F.; investigation, A.F.; resources, R.E.; writing—original draft preparation, A.F.; writing—review and editing, A.F., R.E., and F.A.; visualization, A.F., F.A., and A.N.; supervision, R.E. All authors have read and agreed to the published version of the manuscript.

Funding: This research received no external funding.

Acknowledgments: The writers thank the Director of the Hydraulics Laboratory at Colorado State University for making the flume available for the study.

Conflicts of Interest: The authors declare no conflict of interest.

References

1. Fujita, I.; Muste, M.; Kruger, A. Large-scale particle image velocimetry for flow analysis in hydraulic engineering applications. *J. Hydraul. Res.* **1998**, *36*, 397–414. [CrossRef]
2. Coz, J.L.; Hauet, A.; Pierrefeu, G.; Dramais, G.; Camenen, B. Performance of image-based velocimetry (LSPIV) applied to flash-flood discharge measurements in Mediterranean rivers. *J. Hydrol.* **2010**, *394*, 42–52.
3. Guillén, N.F.; Patalano, A.; García, C.M.; Bertoni, J.C. Use of LSPIV in assessing urban flash flood vulnerability. *Nat. Hazards* **2017**, *87*, 383–394.
4. Al-mamari, M.; Kantoush, S.; Kobayashi, S.; Sumi, T.; Saber, M. Real-Time Measurement of Flash-Flood in a Wadi Area by LSPIV and STIV. *Hydrology* **2019**, *6*, 27.
5. Dramais, G.; Le Coz, J.; Camenen, B.; Hauet, A. Advantages of a mobile LSPIV method for measuring flood discharges and improving stage-discharge curves. *J. Hydro-Environ. Res.* **2011**, *5*, 301–312.
6. Tsubaki, R.; Fujita, I.; Tsutsumi, S. Measurement of the flood discharge of a small-sized river using an existing digital video recording system. *J. Hydro-Environ. Res.* **2011**, *5*, 313–321.
7. Lewis, Q.W.; Lindroth, E.M.; Rhoads, B.L. Integrating unmanned aerial systems and LSPIV for rapid, cost-effective stream gauging. *J. Hydrol.* **2018**, *560*, 230–246.
8. Bieri, M.; Jenzer, J.; Kantoush, S.A.; Boillat, J.-L. Large scale particle image velocimetry applications for complex free surface flows in river and dam engineering. In Proceedings of the 33rd IAHR Congress Water Engineering for a Sustainable Environment, Vancouver, BC, Canada, 9–14 August 2009; pp. 604–611.
9. Fujita, I.; Aya, S. Refinement of LSPIV technique for monitoring river surface flows. *Water Resour.* **2000**, 1–9. [CrossRef]
10. Harpold, A.A.; Mostaghimi, S.; Vlachos, P.P.; Brannan, K.; Dillaha, T. Stream discharge measurement using a large-scale particle image velocimetry (lspiv) prototype. *Am. Soc. Agric. Biol. Eng.* **2006**, *49*, 1791–1805.
11. Theule, J.I.; Crema, S.; Marchi, L.; Cavalli, M.; Comiti, F. Exploiting LSPIV to assess debris-flow velocities in the field. *Nat. Hazards Earth Syst. Sci.* **2018**. [CrossRef]
12. Sturm, T.W. *Open Channel Hydraulics*; McGraw-Hill: Boston, MA, USA, 2001.
13. Muste, M.; Fujita, I.; Hauet, A. Large-scale particle image velocimetry for measurements in riverine environments. *Water Resour. Res.* **2008**, *44*, W00D19. [CrossRef]
14. Muste, M.; Xiong, Z.; Bradley, A.; Kruger, A. Large-Scale Particle Image Velocimetry–a reliable tool for physical modeling. In Proceedings of the ASCE 2000 Joint Conference on Water Resources Engineering and Water Resources Planning & Management, Minneapolis, MN, USA, 30 July–2 August 2000.
15. Meselhe, E.A.; Peeva, T.; Muste, M. Large scale particle Image Velocimetry for low velocity and shallow water flows. *J. Hydraul. Eng.* **2004**, *130*, 937–940. [CrossRef]

16. Aberle, J.; Rennie, C.D.; Admiraal, D.M.; Muste, M. *Experimental Hydraulics: Methods, Instrumentation, Data Processing and Management, Volume II*; Taylor & Francis Group: London, UK, 2017; pp. 35–193. ISBN 978-1-138-03815-8.
17. Chen, K. *Application of Large-Scale Particle Image Velocimetry at the Hydraulics Laboratory of Colorado State University. M.S*; Colorado State University: Fort Collins, CO, USA, 2018.
18. Fudaa-LSPIV. Available online: https://forge.irstea.fr/projects/fudaa-lspiv (accessed on 5 November 2020).
19. Jodeau, M.; Hauet, A.; Coz, J.L.E.; Bercovitz, Y.; Lebert, F.; Edf, D.T.G.; Hhly, U.R. Laboratory and field LSPIV measurements of flow velocities using Fudaa-LSPIV, a free user-friendly software. In Proceedings of the 1st International Symposium and Exhibiton Hydro-Environment Sensors and Software, Madrid, Spain, 1–3 March 2017; pp. 82–86.
20. Wahl, T.L. Refined Energy Correction for Calibration of Submerged Radial Gates. *J. Hydraul. Eng.* **2005**. [CrossRef]
21. Epple, P.; Steppert, M.; Malcherek, A.; Fritsche, M. Theoretical and numerical analysis of the pressure distribution and discharge velocity in flows under inclined sluice gates. In Proceedings of the ASME-JSME-KSME 2019 8th Joint Fluids Engineering Conference, San Francisco, CA, USA, 28 July–1 August 2019. [CrossRef]
22. Hajimirzaie, S.M.; González-Castro, J.A. A New Energy-Based Rating Algorithm for Controlled Submerged Flow at Gated Spillways. In Proceedings of the World Environmental And Water Resources Congress 2016, West Palm Beach, FL, USA, 22–26 May 2016. [CrossRef]
23. Thompson, D.M.; Nelson, J.M.; Wohl, E.E. Interactions between pool geometry and hydraulics. *Water Resour. Res.* **1998**. [CrossRef]
24. Binnie, A.M. The use of a vertical pipe as an overflow for a large tank. *Proc. R. Soc. London Ser. A Math. Phys. Sci.* **1938**. [CrossRef]
25. Hager, W.H. Supercritical Flow in Channel Junctions. *J. Hydraul. Eng.* **1989**. [CrossRef]
26. Hsu, C.-C.; Wu, F.-S.; Lee, W.-J. Flow at 90° Equal-Width Open-Channel Junction. *J. Hydraul. Eng.* **1998**. [CrossRef]
27. Schindfessel, L.; Creëlle, S.; De Mulder, T. Flow patterns in an open channel confluence with increasingly dominant tributary inflow. *Water* **2015**, *7*, 4724–4751. [CrossRef]
28. Nowroozpour, A.; Ettema, R. Observations from contraction-scour experiments conducted with a large rectangular channel. *J. Hydraul. Eng.* under review.
29. Kim, Y. Uncertainty Analysis for Non-Intrusive Measurement of River Discharge Using Image Velocimetry. Ph.D. Thesis, Department of Civil and Environmental Engineering, The University of Iowa, Iowa City, IA, USA, July 2006.
30. Sutarto, T.E. Application of Large-Scale Particle Image Velocimetry (LSPIV) to identify flow pattern in a channel. *Procedia. Eng.* **2015**, *125*, 213–219. [CrossRef]
31. Genc, O.; Ardıçlıoğlu, M.; Ağıralioğlu, N. Calculation of mean velocity and discharge using water surface velocity in small streams. *Flow Meas. Instrum.* **2015**, *41*, 115–120. [CrossRef]